GUCY2D Gene Loss-of-Function Mutations Responsible for Leber Congenital Amaurosis 1

Feng Xue
School of Medicine, Zhejiang University
Tianying Wei
Zhejiang University School of Medicine
Junhui Sun
Zhejiang University School of Medicine
Yuqin Luo
Zhejiang University School of Medicine
Yanan Huo
Zhejiang University School of Medicine
Ping Yu
Zhejiang University School of Medicine
Jiao Chen
Zhejiang University School of Medicine
Xiaoming Wei
BGT-Wuhan
Ming Qi
Zhejiang University School of Medicine
Yinghui Ye (yeyh1999@zju.edu.cn)
Women's Hospital, Zhejiang University School of Medicine https://orcid.org/0000-0001-7520-3871

Research article

Keywords: LCA 1, GUCY2D, catalytic activity, ROS-GC1, cGMP

Posted Date: July 18th, 2019

DOI: https://doi.org/10.21203/rs.2.11649/v1

Abstract

Background: Leber congenital amaurosis (LCA) is a group of severe congenital neurodegenerative diseases. Variants in guanylate cyclase 2D (GUCY2D), which encoded guanylate cyclase protein (ROS-GC1) associate with LCA1, accounting for 6–21% of all LCA cases. Methods: In this study, one family with LCA1 was recruited from China. A combination of next-generation sequencing (NGS) and Sanger sequencing was used for disease-causing mutations screening. Additionally, immunohistochemistry and HPLC-coupled tandem mass-spectrometry (HPLC-MS/MS) were used to confirm the cellular location and catalytic activity of ROS-GC1 mutants, respectively. Results: We found three novel mutations (c.139_139delC, c.835G>A and c.2783G>A) in GUCY2D gene. The results showed that mutation c.139_139delC results in a truncated protein and destroys the structure of ROS-GC1 protein. Mutations c.835G>A and c.2783G>A exert no effects on cellular location, whereas significantly reduce the catalytic activity of ROS-GC1. Conclusions: Our findings highlight the clinical range of LCA. Moreover we used HPLC-MS/MS to analyze the concentration of 3', 5'-cyclic guanosine monophosphate (cGMP), suggesting that HPLC-MS/MS can be an effective alternative method to evaluate the catalytic activity of wild type (wt) and mutant ROS-GC1.

Background

Leber congenital amaurosis (LCA) is the earliest and most severe form of all inherited retinal dystrophies and accounts for at least 5% of all retinal dystrophies [1]. LCA is generally inherited in an autosomal recessive manner [2 - 4], and characterized by genetically and phenotypically heterogeneous. To date, mutations in 20 genes associate with LCA [5]. The distributions of pathogenic genes vary considerably among different populations, however, guanylate cyclase 2D (*GUCY2D*) is a more common LCA gene, *GUCY2D* mutations account for 6%-12% LCA (LCA1) [4, 5].

Guanylate cyclase 1 (ROS-GC1), encoded by *GUCY2D*, is expressed in rod and cone cells of the vertebrate retina, and catalyzes the synthesis of 3', 5'-cyclic guanosine monophosphate (cGMP). ROS-GC1 is negative controlled by Ca^{2+} feedback loop, as decreasing Ca^{2+} increase ROS-GC1 activity and vice versa. However, the effects of Ca^{2+} concentration on ROS-GC1 are not direct, this feedback is regulated by small Ca^{2+}-binding proteins guanylate cyclase-activating proteins (GCAPs), which bind to overlapping binding sites within juxtamembrane domain (JMD), kinase homology domain (KHD) and dimerization domain (DD) of ROS-GC1. In addition to those domains above, ROS-GC1 also possesses leader sequence (LS), extracellular domain (ECD), transmembrane domain (TM) and cyclase catalytic domain (CCD) [6]. Currently, 127 *GUCY2D* mutations can cause LCA1, those disease-causing mutations point to different domain of ROS-GC1, leading to non-functional domain, then result in LCA1 [5]. For example, mutation Pro575Leu, locating at JMD domain, lacks sensitivity to GCAP1 regulation and induces a dysregulation of the Ca^{2+}-sensitive cyclase activation profile. Patients carry mutation Pro575Leu suffer from LCA1 for the distortion of the Ca^{2+}-cGMP homeostasis, subsequently, need more time to restore from the dark [7].

In the present study, next-generation sequencing (NGS) was performed to screen 222 genes that are known to be responsible for 24 kinds of ophthalmic genetic diseases in the proband. After confirming the results by Sanger sequencing, we finally identified three novel variants in *GUCY2D* gene, including c.139_139delC (Ala49Profs*36), c.835G>A (Asp279Asn) and c.2783G>A (Gly928Glu), whereas none of these mutations have been investigated. This study is to address the effects of mutations on ROS-GC1.

Methods

LCA patients

A family with a 5-year-old proband (III-2) and two suspected patients (III-1 and III-3) were recruited for this study. Written informed consent was obtained from each individual to participate in this study. The proband was diagnosed with LCA at Guangdong Zhongshan Hospital, Shanghai General Hospital and the Second Affiliated Hospital of School of Medicine, Zhejiang University. The pedigree was constructed for the proband based on information provided by the guardians.

DNA isolation and qualification

Total genomic DNA was extracted using the Relax Gene Blood DNA System (Tiangen, Beijing, China) in accordance with the manufacturer's instructions. All DNA was dissolved in sterilized double-distilled water and kept at –20 °C until assayed.

DNA degradation and contamination were monitored on 1% agarose gels. All DNA samples were examined for protein contamination (as indicated by the A_{260}/A_{280} ratio) and reagent contamination (indicated by the A_{260}/A_{230} ratio) with a NanoDrop ND 1000 spectrophotometer (NanoDrop, Wilmington, DE, USA).

Next generation sequencing (NGS)

DNA samples obtained from the proband were sequenced using microarray-based next-generation sequencing. A custom Sequence Capture 2.1M Human Array from Roche NimbleGen (Madison, WI, USA) was designed to capture 3093 exons (including 100 bp regions that flanked each side of the exons) from 222 genes known to be associated with common genetic diseases, including Retinitis pigmentosa, Waardenburg syndrome, X-linked juvenile retinoschisis, Crystalline retinitis pigmentosa, Albinism, LCA, Bardet Biedl syndrome and Cone-rod dystrophy (Table 1). The procedure for the preparation of the libraries was consistent with standard operating protocols published previously [8].

Mutation validation by Sanger sequencing

Candidate variants identified by NGS were validated by Sanger sequencing. Primers of the *GUCY2D* gene (NG_009092.1) used in Sanger sequencing were designed by Primer-BLAST (http://www.ncbi.nlm.nih.gov/tools/ primer-blast/), and synthesized by Sangon Biotech (Shanghai, China) (Table 2). All the amplifications were examined by electrophoresis using 2% agarose gels and sequenced by BioSune Biotechnology Co., Ltd. (Shanghai, China). The sequencing results were further compared and analyzed by Mutation Surveyor [9].

Construction of wt and mutant human ROS-GC1 recombination plasmids

The cDNA of human ROS-GC1 was obtained from Gene Copoeia (EX-Z0715-M98). Primers F and R contain XhoI and AgeI were used to amplify ROS-GC1 (Table 3). Vector pEGFP-N1 was cutted by XhoI and AgeI. PCR amplify production was sub-cloned into pEGFP-N1 using ClonExpress (Vazyme, C13) to construct recombined plasmid pEGFP-GC1.

Site-directed mutagenesis PCR was used to construct the mutant ROS-GC1. Primers used in site-directed mutagenesis PCR are shown in Table 3. Each mutant was achieved by two step PCRs using pEGFP-GC1 as template. For c.139_139delC (Ala49Profs*36), two pairs primers F and r-139, R-BamHI and f-139 were used in the first step PCR. F and R-BamHI were used in the second step. For c.835G>A (Asp279Asn), two pairs primers F and r-835, R-BamHI and f-835 were used in the first step PCR. F and R-BamHI were used in the second step. For c.2783G>A (Gly928Glu), primers F-BamHI and r-2783, R and f-2783 were used in the first step PCR. F-BamHI and R were used in the second step. For each mutation, amplification products in the first step were cleaned up (Axygen), mixed, and used as template in the second PCR reaction. All the final PCR amplification were inserted into the digested pEGFP-N1 using ClonExpress.

Recombined plasmids pEGFP-GC1, pEGFP-Ala49Profs*36, pEGFP-Asp279Asn and pEGFP-Gly928Glu were transformed into E.coil DH5a. DNA was prepared by using plasmid DNA purification kit from Macherey-nagel following the manufacturer's instructions. Sequence was verified by Sanger sequencing.

Cellular localization of wt and mutant ROS-GC1 recombination plasmids

pEGFP-N1, pEGFP-GC1, pEGFP-Ala49Profs*36, pEGFP-Asp279Asn and pEGFP-Gly928Glu were transfected into HeLa cells using transfection reagent PolyJet Reagent (SigmaGen). After 36h, cells were washed and fixed in 4% paraformaldehyde. The antibody anti-Na^+/K^+-ATPase (1:100, HuaAn Biotechnology Co.,Ltd) was used to identify the plasma membrane of HeLa cells. Cell nuclei were stained by 4',6-diamidino-2-phenylindole (DAPI, 10μg/ml, Solarbio). The detail operational process was performed as described before [10]. Localization of pEGFP-N1, pEGFP-GC1, pEGFP-Ala49Profs*36, pEGFP-Asp279Asn and pEGFP-Gly928Glu in HeLa cells were observed by Nikon A1R.

Validation of cGMP quantitation by HPLC-MS/MS

HeLa cells were transfected with pEGFP-N1, pEGFP-GC1, pEGFP-Asp279Asn and pEGFP-Gly928Glu. After 36h, cells were collected from 100mm plates and washed three times with PBS. Removed the supernatant carefully, added 300μl of ice-cold extraction medium (acetonitrile/methanol/water, 2/2/1 v/v/v) to each tube. 25ng/ml tenofovir (TNF) was added as internal standard. After dissolving, the sample was frozen in liquid nitrogen for 30s immediately to stop cGMP metabolism, followed by incubating in a 37°C water bath for 60s. After repeating 6 times, samples were heated at 98°C for 20min. Samples were cooled down on ice and centrifuged at 20,000×g 4°C for 10min. The supernatant was transferred into a new tube and the unsolved residue was extracted two more times with 400μl extraction medium. After evaporating, we collected the residues and dissolved it in water for further analyze.

The cGMP concentrations were analyzed via HPLC-MS/MS. The samples were applied to HPLC utilizing ACQUITY CSH-C18 column (1.7μm, 2.1×100mm column, Waters, Ireland). The binary pump system supplied two eluents for chromatographic analysis, eluent A (10mM formic acid) and eluent B (acetonitrile). Flow rate was 0.3ml/min. Analyte detection was conducted on the sensitive triple quadrupole mass spectrometer (Waters TQ-XS, USA). Nitrogen was used as collision gas. 100ng/ml cGMP (G7504, Sigma, Germany) was used as a standard. All the processes were referenced to method described before [11].

Bioinformatics analysis

All the sequences were analyzed by the Mutation Surveyor software and aligned to the NCBI nucleotide sequence of *GUCY2D* (NG_009092.1). The pathogenicity of mutations was evaluated using the in silico predictors SIFT (http://sift.jcvi.org/), PolyPhen-2 (http://genetics.bwh.harvard.edu/pph2/) and Mutation Taster (http://www.mutationtaster.org/). Computational modeling for the mutant ROS-GC1 by Chimera (PDB ID: 1AWL) was used to study the impact of Gly928Glu on the three-dimensional (3D) structure.

Results

Clinical description of the proband

The proband (III-2) was a five-year-old girl who showed visual disorder but could perceive light in a dark room. The proband displayed the classic oculo-digital sign. Ophthalmological examination revealed pendular nystagmus, roving eye movements, macular “colobomas” and optic disc abnormality. Additionally, dim retina and salt-and-pepper pigmentation were found in the fundus. The results of flash visual evoked potential (VEP) showed that the latent period of binocular P-waves was prolonged severely and amplitudes were reduced severely. The electroretinogram (ERG) results showed that the latent period and amplitude of binocular scotopia rod response b-wave, mixed response a-wave and mixed response b-wave were flat. With attenuated photopic 30-Hz flicker, the full-field ERG (ffERG) showed a worsening

delay of the cone-dependent response. The latent period and amplitude of the binocular photopic cone response a-wave and b-wave were flat. Clinical examination confirmed that both parents were unaffected.

GUCY2D mutation analysis

After analyzing the sequencing results of NGS, two novel mutations c.139_139delC and c.2783G>A of the *GUCY2D* gene were identified in the proband (III-2). The presence of c.139_139delC and c.2783G>A in other family members was confirmed by Sanger sequencing. The sequencing results show that II-2 and II-3 are heterozygous mutation carriers possess c.139_139delC and c.2783G>A, respectively (Fig. 1B1, 2).

III-3 was described as an LCA1 patient (Fig. 1A). The *GUCY2D* gene sequences of the suspected patient's sibling (III-4) and parents (II-7 and II-8) were determined by Sanger sequencing. The results show that II-7 is a c.2783G>A mutation carrier, and II-8 possesses another novel mutation c.835G>A (Fig. 1B3). The sibling (III-4) possesses no *GUCY2D* mutation.

Prediction of the pathogenic effect of ROS-GC1 mutations

Ala49Profs*36, Asp279Asn and Gly928Glu are located at LS, ECD and CCD domain of ROS-GC1, respectively (Fig. 2C). By analyzing the three mutations by SIFT, PolyPhen-2 and Mutation Taster, we propose that c.835G>A (SIFT: damaging, score: 0.01; PloyPhen-2: probably damaging, score: 1.00; Mutation Taster: disease causing), c.2783G>A (SIFT: damaging, score: 0.00; PloyPhen-2: probably damaging, score: 1.00; Mutation Taster: disease causing) and c.139_139delC (Mutation Taster: disease causing) are disease-causing mutations. Additionally, multiple sequence alignments show that aspartic acid and glycine at positions 279 and 928 are highly conserved across species (Additional Fig. 1) indicating that Asp279 and Gly928 exert important roles in ROS-GC1, mutations located at 279 and 928 are more likely to cause disease.

The high-resolution 3D structure of full-length ROS-GC1 remains unsolved. The theoretical model (PDB ID: 1AWL) which contains 158 amino acids from 871 to 1028 was used to study the impact of c.2783G>A (Gly928Glu) on the 3D structure of ROS-GC1. As shown in Fig. 2, the residue of Glu directly connects to GTP, decreases the internal space of catalytic core, changes the relative position of GTP and catalytic core, furthermore reduces the binding capabilities and the catalytic activity of ROS-GC1.

Localization of wt and mutant ROS-GC1

pEGFP-N1, pEGFP-GC1, pEGFP-Ala49Profs*36, pEGFP-Asp279Asn and pEGFP-Gly928Glu were transfected into HeLa cells after verification by Sanger sequencing (Additional Fig. 2). Immunofluorescence was used to confirm the localization of wt and mutant ROS-GC1. In HeLa cells, wt and mutant ROS-GC1 were co-express with EGFP (Fig. 3, top panels). Anti-Na^+/K^+-ATPase antibody was used as specific markers for plasma membrane (Fig. 3, second panels). DAPI was used to stain nuclei

(Fig. 3, third panels). No Ala49Profs*36 can be observed in Fig. 3 (bottom panels). We propose Ala49Profs*36 results in severely damaged of ROS-GC1 and causes a completely inactive of ROS-GC1. The localizations of Asp279Asn and Gly928Glu are similar to wt ROS-GC1.

Catalytic features of wt and mutant ROS-GC1

HPLC-MS/MS was used to analyze cGMP concentrations in HeLa cells. The cGMP concentration in cells transfected pEGFP-N1 was undetectable. In contrast, the cGMP concentration in cells transfected pEGFP-GC1 was about 3.631pmol/ml. Compared to wt, cells transfected pEGFP-Asp279Asn and pEGFP-Gly928Glu, showed significantly lower concentrations of cGMP (Fig. 4A), implying that Asp279Asn and Gly928Glu significantly reduced the catalytic activity of ROS-GC1. In addition, Gly928Glu disrupted the catalytic activity of ROS-GC1 more severely, consistent with the bioinformatics analysis results. Moreover, all the missense mutations exerted no significant effect on the expression level of ROS-GC1 (Fig. 4B).

Discussion

Over the years, 20 known genes associated with LCA have been identified. The large number of genes and exons, and the lack of mutational hot spots make individual screening for disease-causing mutations by Sanger sequencing become difficult and expensive. However, NGS technologies provide more convenient and effective strategies to screen for pathogenic genes [12 - 14]. In this study, a family with the one proband and two deceased suspect LCA patients was analyzed. By testing all the samples, three mutations (c.139_139delC, c.2783G>A and c.835G>A) in *GUCY2D* gene were found, and all mutations have not been documented by 1000 Genomes Projects yet.

The novel disease-causing mutation c.139_139delC (Ala49Profs*36) carried by II-1, II-2 and III-3 generates a truncated protein (83 amino acids), only contains a part of LS domain (Fig. 2C). As all domains of ROS-GC1 deletion, the truncated protein generated by Ala49Profs*36 is extremely unstable, thereby the enzymatic activity is abolished and the cGMP production will be completely insufficient. Subsequently, the absence of cGMP consistently results in photoreceptor cell polarization, which finally leads to vision loss.

Multiple sequence alignments indicated that aspartic acid and glycine at positions 279 and 928 are highly conserved across species. Those residues are important to protein function. As mutations located at ECD domain affect the function of ROS-GC1 by decreasing cGMP production and result in LCA1 [15], in according with our finding that mutation Asp279Asn, which located at ECD domain, significantly decreases catalytic activity of ROS-GC1. However, Asp279Asn mutant does not alter the cellular localization and the expression level of ROS-GC1. Mutant c.2783G>A (Gly928Glu) is located at the catalytic domain of ROS-GC1 [16]. Bioinformatics analysis was used to estimate the effects of Gly928Glu on catalytic activity of ROS-GC1. Different from Gly928, the amino acid residue of Glu928 directly connects to the substrate GTP. The change of internal space of catalytic core perturbs the catalytic activity of ROS-GC1. In order to make the experiment more reliable and convincing, HPLC-

MS/MS was used to confirm the effects of missense mutations on the ROS-GC1 activity. Results from HPLC-MS/MS show that mutations Asp279Asn and Gly928Glu decrease the ROS-GC1 activity significantly, especially Gly928Glu, consistent with 3D-model analysis result and bioinformatics analysis results of SIFT, PloyPhen-2 and Mutation Taster. In contrast, Gly928Glu shares the similar characteristics as wt ROS-GC1, including cellular localization and ROS-GC1 expression level.

Conclusions

In this study, we found three novel mutations (c.139_139delC, c.2783G>A and c.835G>A) in *GUCY2D* gene. Mutation c.139_139delC results in a truncated protein, losing all domains of ROS-GC1. Although mutations c.835G>A and c.2783G>A show normal protein expression level and subcellular localization, both mutations significantly reduce the catalytic activity of ROS-GC1. Instead of using radioisotopes labeling, HPLC-MS/MS was used to analysis cGMP concentrations in this study. Compared to the traditional method, HPLC-MS/MS is more convenient, it can be an effective alternative method to evaluate the content of cGMP.

Abbreviations

LCA: Leber congenital amaurosis; *GUCY2D*: guanylate cyclase 2D; ROS-GC1: guanylate cyclase protein 1; GCAPs: guanylate cyclase-activating proteins; CCD: cyclase catalytic domain; DD: dimerization domain; ECD: extracellular domain; JMD: juxtamembrane domain; KHD: kinase homology domain; LS: leader sequence; TM: transmembrane domain; HPLC-MS/MS: HPLC-coupled tandem mass-spectrometry; wt: wild type; NGS: next-generation sequencing

Declarations

Ethics approval and consent to participate

All procedures performed were in accordance with the Declaration of Helsinki and approved by the ethical standards of the Institutional Review Board, Zhejiang University. Written informed consent was obtained from all individuals who participated in this study and the parent of children under 16.

Consent to publish

not applicable.

Availability of data and materials

The data used and analyzed in this study are available from the corresponding author.

Competing of interests

The authors report no conflict of interests.

Funding

The study was supported by grants from the National Natural Science Foundation of China (81771585 31371271, 81200662), National Key R&D Program of China 2018YFC1004900 and the Natural Science Foundation of Zhejiang Province (LZ14C060001, LY12H12010). In this research, t he funding organization exerted no role in the design or conduct.

Authors' contributions

P.Y. and Y.H.Y. designed the experiment, X.F., T.Y.W and J.H.S. performed the experiment and analyzed the data, Y.N.H., J.C. and X.M.W. recruited the proband and the family members, X.F. and T.Y.W. write the paper, Y.H.Y and M.Q. modified the paper. All the authors approved the final manuscript.

Acknowledgements

The authors wish to thank the patient and his family for their cooperation and participation in the study.

References

1. Perrault I, Rozet JM, Gerber S, Ghazi I, Leowski C, Ducroq D, Souied E, Dufier JL, Munnich A, Kaplan J. Leber congenital amaurosis. Molecular genetics and metabolism 1999; 68:200-8.

2. Cremers FP, van den Hurk JA, den Hollander AI: Molecular genetics of Leber congenital amaurosis. Human molecular genetics2002; 11:1169-76.

3. Kaplan J, Bonneau D, Frezal J, Munnich A, Dufier JL. Clinical and genetic heterogeneity in retinitis pigmentosa. Human genetics1990; 85:635-42.

4. den Hollander AI, Roepman R, Koenekoop RK, Cremers FP. Leber congenital amaurosis: genes, proteins and disease mechanisms. Progress in retinal and eye research 2008; 27:391-419.

5. Chacon-Camacho OF, Zenteno JC. Review and update on the molecular basis of Leber congenital amaurosis. World journal of clinical cases2015; 3:112-24.

6. Sharon D, Wimberg H, Kinarty Y, Koch KW. Genotype-functional-phenotype correlations in photoreceptor guanylate cyclase (GC-E) encoded by GUCY2D. Progress in retinal and eye research2018; 63:69-91.

7. Zagel P, Koch KW. Dysfunction of outer segment guanylate cyclase caused by retinal disease related mutations. Frontiers in molecular neuroscience2014; 7:4.

8. Head SR, Komori HK, LaMere SA, Whisenant T, Van Nieuwerburgh F, Salomon DR, Ordoukhanian P. Library construction for next-generation sequencing: overviews and challenges. BioTechniques2014; 56:61-64, 66, 68, passim.

9. Ho Duy B, Zhytnik L, Maasalu K, Kandla I, Prans E, Reimann E, Martson A, Koks S. Mutation analysis of the COL1A1 and COL1A2 genes in Vietnamese patients with osteogenesis imperfecta. Human genomics2016; 10:27.

10. Zagel P, Dell'Orco D, Koch KW. The dimerization domain in outer segment guanylate cyclase is a Ca(2)(+)-sensitive control switch module. Biochemistry2013; 52:5065-74.

11. Beckert U, Aw WY, Burhenne H, Forsterling L, Kaever V, Timmons L, Seifert R. The Receptor-Bound Guanylyl Cyclase DAF-11 Is the Mediator of Hydrogen Peroxide-Induced cGMP Increase in Caenorhabditis elegans [corrected]. PloS one 2013; 8:e72569.

12. Siu LL, Conley BA, Boerner S, LoRusso PM. Next-Generation Sequencing to Guide Clinical Trials. Clinical cancer research : an official journal of the American Association for Cancer Research 2015; 21:4536-44.

13. Nuytemans K, Vance JM. Whole exome sequencing. Rinsho shinkeigaku = Clinical neurology 2010; 50:952-55.

14. Ng SB, Buckingham KJ, Lee C, Bigham AW, Tabor HK, Dent KM, Huff CD, Shannon PT, Jabs EW, Nickerson DA *et al.* Exome sequencing identifies the cause of a mendelian disorder. Nature genetics2010; 42:30-35.

15. Tucker CL, Ramamurthy V, Pina AL, Loyer M, Dharmaraj S, Li Y, Maumenee IH, Hurley JB, Koenekoop RK. Functional analyses of mutant recessive GUCY2D alleles identified in Leber congenital amaurosis patients: protein domain comparisons and dominant negative effects. Molecular vision2004; 10:297-303.

16. Liu Y, Ruoho AE, Rao VD, Hurley JH. Catalytic mechanism of the adenylyl and guanylyl cyclases: modeling and mutational analysis. Proceedings of the National Academy of Sciences of the United States of America 1997; 94:13414-19.

Figure Legends And Additional Files

Fig. 1 Brief information of *GUCY2D* mutations in the LCA1 family. A: Pedigree of the LCA1 family. ↗ represents the proband, □ represents the normal male, ● represents the normal female, crossed symbols represent the deceased subject. ● and ■ denotes patients, the half-shaded icons denote the mutation carriers as =c.139_139delC, =c.2783G>A, and =c.835G>A. B: 1: The sequencing results of the family show

the mutation c.139_139delC, indicated by the arrows. 2: The sequencing results of the family show the mutation c.2783G>A, indicated by the arrows. 3: The sequencing result of the family member II-8 with mutation c.835G>A; forward sequencing result (top), reverse sequencing result (bottom).

Fig. 2 The protein domains and Modeling analysis of mutation Gly928Glu. A: 3D-modeling analysis of the Gly928. B: 3D-modeling analysis of the Glu928. Green line indicates ROS-GC1 residue. C: ROS-GC1 domains and location of Ala49Profs*36, Asp279Asn and Gly928Glu.

Fig. 3 Cellular localization of wt and mutant ROS-GC1 in HeLa cells. Wt and mutant ROS-GC1 were co-expression with EGFP. For immunostaining, (top panels) anti-EGFP as markers for EGFP, wt and mutant ROS-GC1, (second panels) anti-Na^+/K^+-ATPase was used as cell membrane marker, (third panels) DAPI was used as nuclear marker, (bottom panels) overlay of EGFP or wt and mutant ROS-GC1, membrane localization and nucleus. The scale bar is 10μm.

Fig. 4 cGMP concentrations and ROS-GC1 expression levels in HeLa cells. A: Transfected HeLa cells with pEGFP-N1, pEGFP-GC1, pEGFP-Asp279Asn and pEGFP-Gly928Glu. Cells solution was collected and used to estimate cGMP concentrations. P-values were calculated by means of independent sample T-test. ***: p value≤0.001. B: Western blot of HeLa cells expressing human EGFP, wt and mutant ROS-GC1.

Additional Fig. 1 Multiple sequence alignment of ROS-GC1 from different species reveals that codon 279 and 928, where the mutations (Asp279Asn and Gly928Glu) occurrs, are located within a highly conserved region.

Additional Fig. 2 The sequencing results of wt and mutant *GUCY2D*. Sanger sequencing was used to verify the sequence of recombination plasmid pEGFP-GC1, pEGFP-Ala49Profs*36, pEGFP-Asp279Asn and pEGFP-Gly928Glu.

Figures

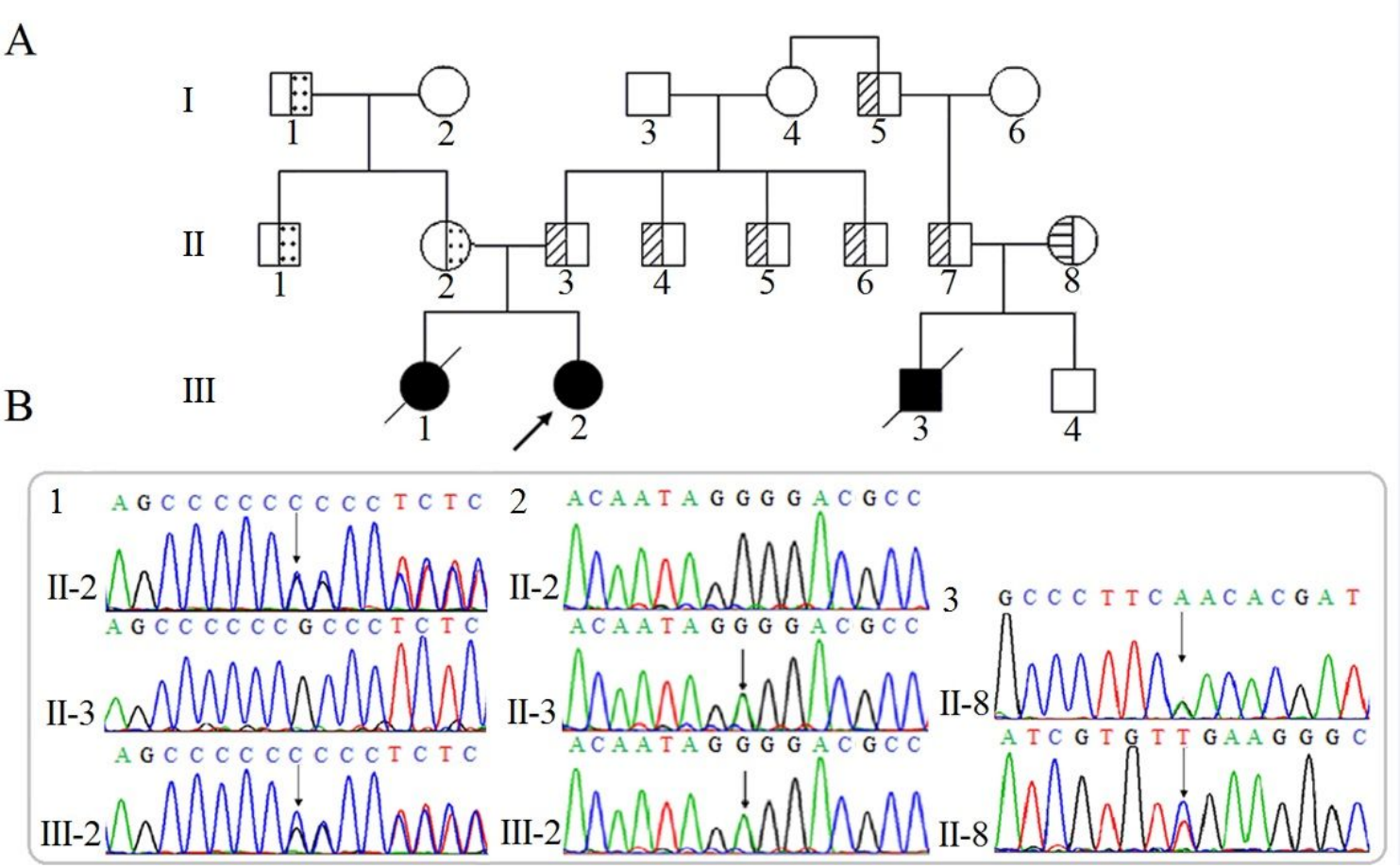

Figure 1

Brief information of GUCY2D mutations in the LCA1 family. A: Pedigree of the LCA1 family. ↗ represents the proband, □ represents the normal male, ● represents the normal female, crossed symbols represent the deceased subject. ● and ■ denotes patients, the half-shaded icons denote the mutation carriers as =c.139_139delC, =c.2783G>A, and =c.835G>A. B: 1: The sequencing results of the family show the mutation c.139_139delC, indicated by the arrows. 2: The sequencing results of the family show the mutation c.2783G>A, indicated by the arrows. 3: The sequencing result of the family member II-8 with mutation c.835G>A; forward sequencing result (top), reverse sequencing result (bottom).

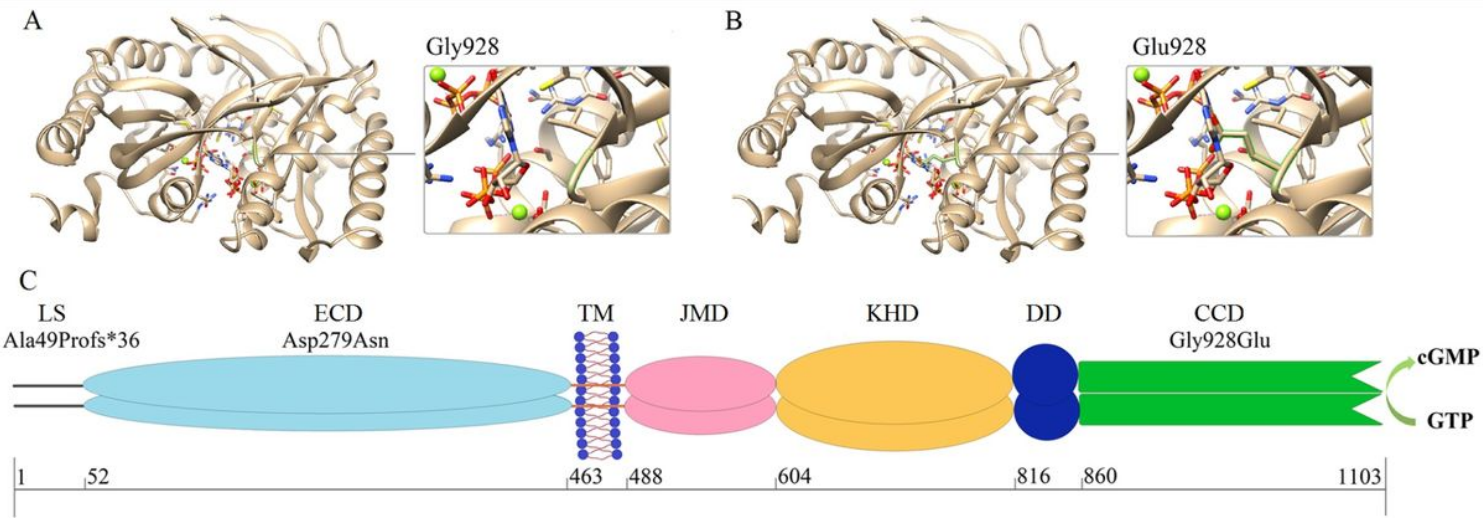

Figure 2

The protein domains and Modeling analysis of mutation Gly928Glu. A: 3D-modeling analysis of the Gly928. B: 3D-modeling analysis of the Glu928. Green line indicates ROS-GC1 residue. C: ROS-GC1 domains and location of Ala49Profs*36, Asp279Asn and Gly928Glu.

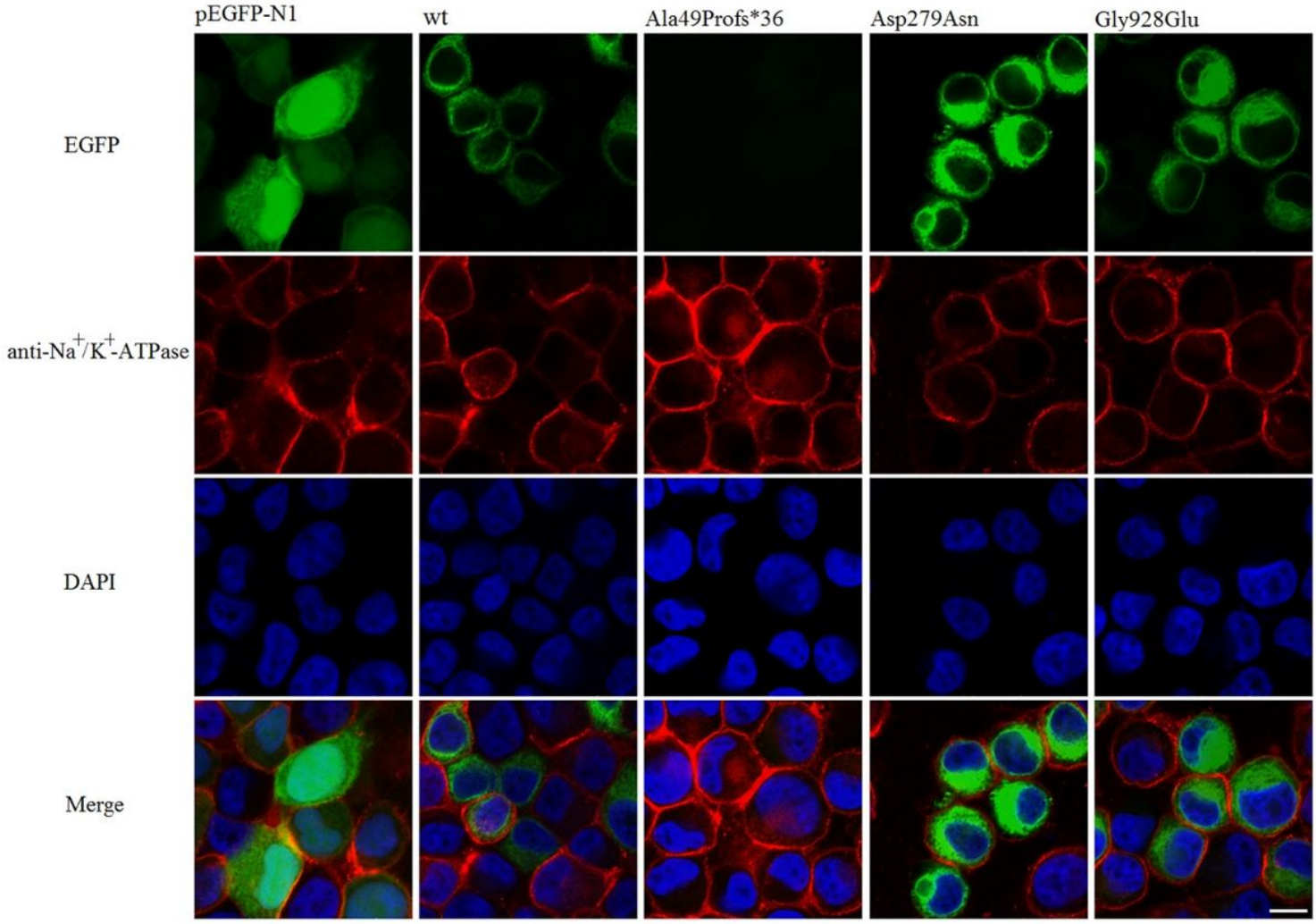

Figure 3

Cellular localization of wt and mutant ROS-GC1 in HeLa cells. Wt and mutant ROS-GC1 were co-expression with EGFP. For immunostaining, (top panels) anti-EGFP as markers for EGFP, wt and mutant ROS-GC1, (second panels) anti-Na+/K+-ATPase was used as cell membrane marker, (third panels) DAPI was used as nuclear marker, (bottom panels) overlay of EGFP or wt and mutant ROS-GC1, membrane localization and nucleus. The scale bar is 10μm.

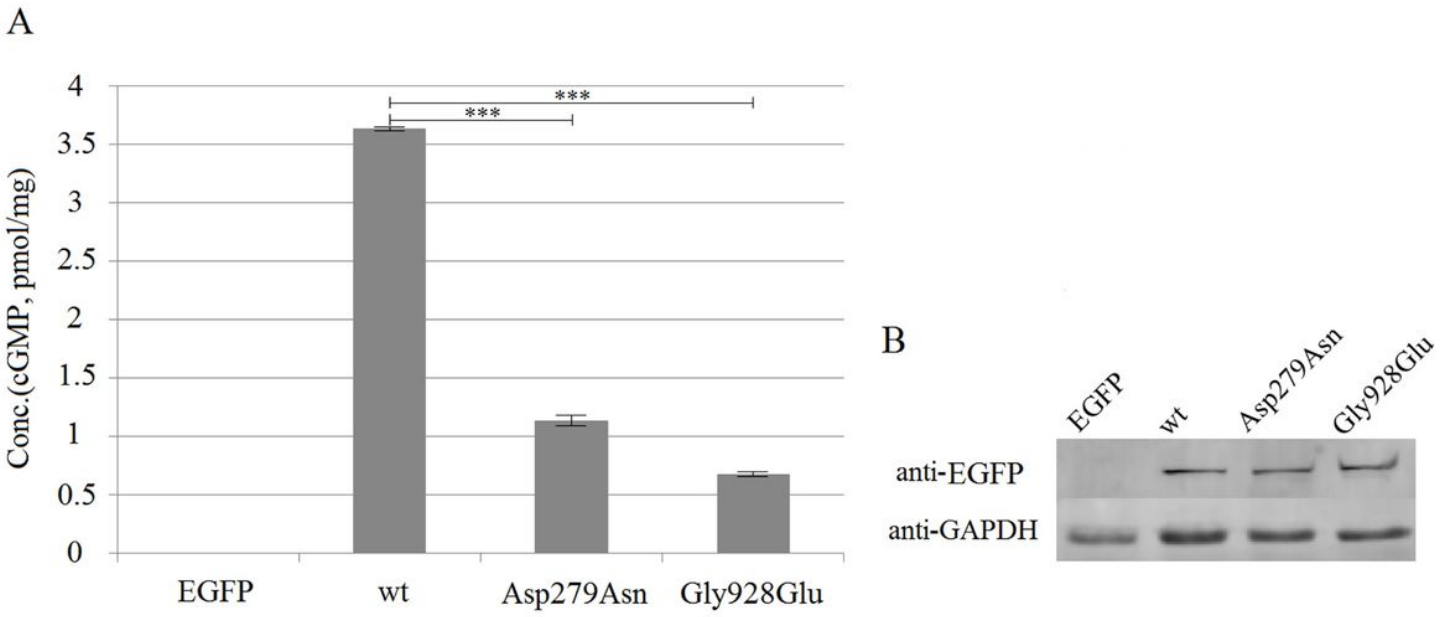

Figure 4

cGMP concentrations and ROS-GC1 expression levels in HeLa cells. A: Transfected HeLa cells with pEGFP-N1, pEGFP-GC1, pEGFP-Asp279Asn and pEGFP-Gly928Glu. Cells solution was collected and used to estimate cGMP concentrations. P-values were calculated by means of independent sample T-test. ***: p value≤0.001. B: Western blot of HeLa cells expressing human EGFP, wt and mutant ROS-GC1.

Supplementary Files

This is a list of supplementary files associated with this preprint. Click to download.

- supplement1.pdf
- supplement2.jpg
- supplement3.pdf
- supplement4.pdf
- supplement5.jpg